EUROPEAN ORGANIZATION FOR NUCLEAR RESEARCH
CERN-PPE/94-124
June 30, 1994

Precision Measurement of Electroweak Parameters from the Scattering of Muon-Neutrinos on Electrons

The CHARM II Collaboration

P. Vilain[1], G. Wilquet[1]
Inter-University Institute for High Energies (ULB-VUB), Brussels, Belgium

R. Beyer, W. Flegel, H. Grote, T. Mouthuy[2], H. Øveras, J. Panman, A. Rozanov[3], K. Winter, G. Zacek, V. Zacek
CERN, Geneva, Switzerland

F. W. Büsser, C. Foos, L. Gerland, T. Layda[4], F. Niebergall, G. Rädel[5], P. Stähelin, T. Voss
II. Institut für Experimentalphysik[6], Universität Hamburg, Germany

D. Favart, G. Grégoire, E. Knoops[7], V. Lemaître
Université Catholique de Louvain, Louvain-la-Neuve, Belgium

P. Gorbunov, E. Grigoriev, V. Khovansky, A. Maslennikov
Institute for Theoretical and Experimental Physics, Moscow, Russian Federation

W. Lippich, A. Nathaniel, A. Staude, J. Vogt
Sektion Physik[6] der Universität München, Germany

A.G. Cocco, A. Ereditato, G. Fiorillo, F. Marchetti-Stasi, V. Palladino, P. Strolin
Università and Istituto Nazionale di Fisica Nucleare (INFN), Naples, Italy

A. Capone, D. De Pedis, U. Dore, A. Frenkel-Rambaldi, P.F. Loverre, D. Macina, G. Piredda, R. Santacesaria
Università 'La Sapienza' and Istituto Nazionale di Fisica Nucleare (INFN), Rome, Italy

E. Di Capua, S. Ricciardi, B. Saitta
Università di Ferrara and Istituto Nationale di Fisica Nucleare (INFN), Ferrara, Italy

B. Akkus[8], E. Arik[8], M. Serin-Zeyrek, R. Sever, P. Tolun
High Energy Physics Research Centre, YEFAM, Ankara, Turkey

K. Hiller, R. Nahnhauer, H.E. Roloff
DESY - Institut für Hochenergiephysik, Zeuthen, Germany

(Submitted to Physics Letters B)

Abstract

We report final results on electroweak parameters from muon-neutrino electron scattering observed in the CHARM II detector from 1987 till 1991. In total 2677±82 and 2752±88 neutrino-electron scattering events have been detected in the ν and $\bar{\nu}$-beam, respectively. From the ratio of differential cross sections we obtain for the electroweak mixing angle $\sin^2\theta_{\nu e} = 0.2324 \pm 0.0083$. From the absolute neutrino-electron scattering event rate we determined the effective vector and axial-vector neutral current coupling constants to be $g_V^{\nu e} = -0.035 \pm 0.017$ and $g_A^{\nu e} = -0.503 \pm 0.017$.

---

1 National Foundation for Scientific Research, Belgium
2 now at Centre de Physique des Particules de Marseille, Faculté de Luminy, Marseille, France
3 on leave of absence from ITEP, Moscow, Russian Federation
4 now at University of California at Santa Cruz, USA
5 now at DESY, Hamburg, Germany
6 supported by the German Bundersministerium für Forschung und Technologie (BMFT), under contract numbers 05-5HH22P and 05-5MU12P
7 Inter-University Institute for Nuclear Science, Belgium
8 Bogaziçi Univ., Istanbul, Turkey

1. Introduction

The study of muon-neutrino and muon-antineutrino scattering on electrons has provided results which are crucial for the understanding of the neutral current weak interaction. The observation of one event in 1973 [1] was a corner stone in the discovery of this new interaction. The first quantitative study by the CHARM Collaboration based on 200 events [2] led to a determination of the axial vector coupling g_A^e of the electron to the Z. A value close to $-\frac{1}{2}$ was found lending strong support to a local internal symmetry under which the leptons transform as doublets. The CHARM II experiment aimed at an increase of statistics by an order of magnitude to investigate higher order contributions, so-called radiative corrections. We are reporting in this letter the final data sample collected in the years 1987 to 1991.

We determined the differential cross sections of muon-neutrino and muon-antineutrino scattering on electrons. Within the framework of the electroweak theory t'Hooft [3] has derived the expression for the cross section.

$$\frac{d\sigma_{\bar{\nu}}^{\nu}}{dy} = \frac{G_F^2 s}{4\pi} \left[(g_V \pm g_A)^2 + (g_V \mp g_A)^2 (1-y)^2 \right] \qquad (1)$$

where $s = 2m_eE_\nu$, $y = E_e/E_\nu = (1 - \cos\theta^*)/2$ and θ^* is the c.m. scattering angle, g_V and g_A are the vector and axial vector electron-Z couplings. The neutrino beams contain muon-neutrinos and a small contamination of electron-neutrinos. For electron-neutrinos there is an additonal term, $(2 + g_V + g_A)^2$. It is accounting for the interference of neutral and charged current contributions. About 10% of the neutrino-electron scattering events were induced by electron-neutrinos. From the simultaneous measurement of $d\sigma/dy$ for $\nu_\mu e$ and $\bar{\nu}_\mu e$ and for $\nu_e e$ and $\bar{\nu}_e e$ scattering we derived g_A and g_V with a two-fold sign ambiguity. Results from experiments on $e^+e^- \rightarrow e^+e^-$ annihilation have also a two-fold sign ambiguity. Taken together they select a single solution.

We have already published results on the shapes of the differential cross sections [4]. They are sensitive to the handedness of the electrons on which the neutrinos scatter. While the charged current weak interaction distinguishes left- from right-handed particles, violating parity maximally, we showed that the Z couples to both left- and right-handed electrons, although with different strength as predicted by the theory. We also gave the first experimental evidence for flavour universality of neutrino couplings with the Z, a crucial input for the determination of the number of light neutrino families from the properties of the Z pole [5]. Limits on Z' states and on electromagnetic properties of muon-neutrinos will be published in forthcoming papers.

The detector was conceived to study neutrino-electron scattering [6]. It consists of a massive target calorimeter (692 t) followed by a muon spectrometer. The calorimeter has low density and is instrumented with streamer tubes equiped with digital and analog readout to measure both the energy and the direction of particles produced. This detector was exposed to the horn focused wide band neutrino beam at CERN. Neutrinos were produced by a 450 GeV proton beam accelerated in the Super Proton Synchrotron (SPS) for $2.5 \cdot 10^{19}$ protons on target. Approximately 10^8 neutrino interactions occurred in the detector. Data were collected from 1987-1991. Results based on partial samples have already been published previously [7-9].

The signature of neutrino-electron scattering is a single, forward scattered electron producing an electromagnetic shower in the calorimeter. Low Z material (glass) was chosen for the target calorimeter to ensure good angular resolution for electron showers [10]. Candidate events with electron energies between 3 and 24 GeV were selected. Electron and pion induced showers were discriminated by their characteristic different width. The variable $E_e\,\theta_e^2$, the product of electron energy and the square of the scattering angle, is kinematically constrained to values smaller than 1 MeV. This fact is used to separate neutrino electron scattering from the background of semileptonic events which has a broad distribution.

2. Analysis

We followed the analysis method which was described in detail in a previous publication [9], concerning event selection, neutrino flux measurement and the simultaneous fit of the modelled distributions of events as a function of the invariant $E_e\,\theta_e{}^2$ (see figure 1) and of E_e. The experimental data and the result of the fit is shown in figure 1; the bin size has been chosen according to the experimental resolution.

2677 ± 82 events in the ν beam and

2752 ± 88 events in the $\bar{\nu}$ beam

are attributed to neutrino-electron scattering.

We have made an experimental verification of the modelling of the background processes. The background consists of single π° production by neutral current neutrino interaction (π°) and of quasi-elastic scattering of electron neutrinos on nucleons (qe). A small background of inclusive production of electromagnetic showers is not shown in figure 1 but was taken into account in the fit. A shower induced by a photon yields an even number of charged particles while electron induced showers yield odd numbers. The characteristic difference between electron and photon induced showers is best observed in an early stage of shower development [11]. The analysis of one sample was therefore restricted to those events starting in glass plates directly followed by a scintillator plane. We ensured that detected particles should have traversed the full thickness (3cm) of a scintillation counter by requiring that the reconstructed impact point of the shower is at least 1cm away from the edges of the counter and at least 5cm away from its ends. The scintillation counters covered every fifth module of the target calorimeter. Each counter was composed of twenty 15cm wide and 3cm thick elements. The geometrical acceptance of this selection compared to the standard fiducial volume is 14.7%. In the event selection one and only one of the counter element was allowed to be hit by a shower starting in the glass plate preceding it. The efficiency for this selection is different for π° production (π°) and quasi-elastic ν_e scattering (qe); the values are given as ε_{scin} in table 1. The scintillator pulse heights were corrected for light attenuation and for the signal amplification of the individual counter.

The most probable energy loss of a single electron traversing one scintillation counter is 5 MeV. We selected events associated with a single electron by requiring an energy loss of less than 8 MeV. The efficiency calculated by Monte Carlo methods for detecting the processes is given as ε_8 in table 2, separately for the neutrino and the antineutrino beam.

The background composition for the region $5 < E\theta^2 < 72$ MeV can be described by two equations; one equation holds for the candidate sample

$$N^{data} = N^{\pi^\circ} + N^{qe} \quad , \tag{2}$$

the other applies for selected events with less than 8 MeV energy loss in a scintillation counter element,

$$N_8^{data} = \varepsilon_8^{\pi^\circ} N^{\pi^\circ} + \varepsilon_8^{qe} \; N^{qe} \tag{3}$$

Solving these two equations for N^{π° and N^{qe} we obtained the values given in table 2. The errors are due to the uncertainty of the efficiencies and the event statistics. The result can be expressed in the form of background ratios for the reference region. In order to obtain the background ratio in the candidate sample, R_{bg}, one has to correct for the different selection efficiency of π° and quasi-elastic ν_e events (table 1).

$$R_{bg} = \frac{N^{qe}}{N^{\pi^\circ}} \; \frac{\varepsilon_{scin}^{\pi^\circ}}{\varepsilon_{scin}^{qe}} \tag{4}$$

The corrected ratios for the neutrino and antineutrino beam are given in table 2, together with the ratios R_{bg}^{fit} obtained from the fit of the modelled distributions in figure 1. The two background ratios are in agreement and confirm the modelling of the background distributions.

Another use of the energy loss information in the scintillation counters was to define for each candidate event the probability to be due to a single electron. Classifying the events according to their electron probability we obtained a sample enriched in neutrino-electron scattering events. The signal to background ratio of this sample is improved by a factor of about 3.5 (see figure 2).

3. Results

Turning now to the determination of g_A and g_V we used the samples with and without energy loss information, to reduce the statistical error. Moreover, the absolute normalisation of neutrino fluxes and the presence of ν_ee and $\bar{\nu}_e$e events detected in the same experiment was used to reduce the well known fourfold ambiguity of g_A and g_V to two solutions.

We calculated the ratio of ν_e and $\bar{\nu}_e$ fluxes with respect to the dominant ν_μ and $\bar{\nu}_\mu$ fluxes using Monte Carlo methods and measurements of pion and kaon production [12]. The agreement of the ratio of quasi-elastic ν_e scattering and single π° production determined from the energy loss in a scintillation hodoscope counter and from the fit of the modelled distributions in figure 1 is lending support to this flux evaluation.

The 67% confidence domains of g_A and g_V thus determined from the absolute differential cross sections of ν_μ e, $\bar{\nu}_\mu$e and ν_ee, $\bar{\nu}_e$e scattering are shown in figure 3. They are intersecting each other in two regions of g_A and g_V. Also shown in figure 3 are two cones of values determined by experiments on the forward-backward asymmetry in $e^+e^- \to e^+e^-$ annihilations at LEP [13]. These two solutions are selected out of eight possible cones by the results on e^+e^- annihilations to lepton pairs off the Z pole at PETRA and PEP [15]. For clarity we do not display the results on the Z decay width to e^+e^-, Γe, which define a ring of possible g_A and g_V values. Contributions to the systematic errors are given in table 3. One of the cones is intersecting one of the two solutions of neutrino electron scattering from the CHARM II experiment; this single solution is in agreement with $g_A^e = -\frac{1}{2}$:

$$g_V^{\nu e} = -0.035 \pm 0.012 \text{ (stat)} \pm 0.012 \text{ (syst)} \quad ,$$

$$g_A^{\nu e} = -0.503 \pm 0.006 \text{ (stat)} \pm 0.016 \text{ (syst)} \quad .$$

This had been demonstrated already in 1984 by combining results from the CHARM experiment [2], from $\overline{\nu}_e e$ scattering at a Nuclear Reactor [14] and from experiments on $e^+e^- \to \mu^+\mu^-$ events at PETRA and PEP [15]. It should be remembered that $g_A^{\nu e}$ and $g_V^{\nu e}$ are the product of $g_A^{\nu_\mu} \cdot g_A^e$ and $g_V^{\nu_\mu} \cdot g_V^e$ [5]. As a convention, the sign and the value of $g_A^{\nu_\mu} = g_V^{\nu_\mu} = +\frac{1}{2}$ is assumed.

The neutral current couplings g_A^e and g_V^e derived from neutrino electron scattering and from $e^+e^- \to \ell^+\ell^-$ annihilation studies at LEP [13] surprisingly agree ,within the errors, as shown in figure 4, despite the large difference of energy scales, $Q^2 \sim 0.01$ GeV^2 (for $\nu_\mu e$) and $Q^2 \sim 10^4$ GeV^2 (for e^+e^-). The agreement seems to occur because of the near cancellation of two large higher order terms arising from γ - Z mixing and from the neutrino charge radius. The magnitude of the first term depends on the top quark mass and the cancellation is therefore indeed surprising [16].

Constraining only the relative neutrino to antineutrino flux in the fit of the data we determined from the ratio of $\nu_\mu e$ and $\overline{\nu}_\mu e$ differential cross sections the value of the electroweak mixing angle. From the combined sample we obtained

$$\sin^2 \theta_{\nu e} = 0.2324 \pm 0.0058 \text{ (stat)} \pm 0.0059 \text{ (syst)} \ .$$

This value is in very good agreement with the results obtained at LEP [13].

In conclusion, this high precision experiment on neutrino electron scattering has provided clear experimental support for local internal gauge symmetry as the principle underlying the unification of the weak and electromagnetic interactions, for flavour universality of neutrino-Z coupling, and for a cancellation of radiative corrections involving a particular range of values of the top quark mass.

Acknowledgements

We gratefully acknowledge the help of our many technical collaborators who have contributed to the realisation and the operation of the detector. We are grateful for the grants from the Inter-University Institute for Nuclear Sciences (Belgium), CERN (Geneva, Switzerland), the Bundesministerium für Forschung und Technologie (FRG), the Institute of Theoretical and Experimental Physics (Moscow, Russian Federation), the Istituto Nazionale di Fisica Nucleare (Italy), and the Turkish Scientific and Technical Research Council (TUBITAK); which made the experiment possible. We should like to thank the CERN SPS operating crew and the neutrino beam staff for their competent assistance ensuring the excellent performance of their facilities.

Table 1
Efficiency of scintillator event selection

events	ε_{scin}
π°	$(82.5 \pm 2.8)\%$
qe	$(76.7 \pm 1.6)\%$

Table 2
Efficiency of E < 8MeV selection, events and background ratios

	ν beam	$\bar{\nu}$ beam
ε_8^{qe}	0.561 ± 0.022	0.582 ± 0.027
$\varepsilon_8^{\pi^{\circ}}$	0.103 ± 0.009	0.102 ± 0.009
N^{data}	3886	4996
N_8^{data}	609	855
$N^{\pi^{\circ}}$	3430 ± 102	4276 ± 121
N^{qe}	456 ± 87	720 ± 106
R_{bg}	0.14 ± 0.03	0.18 ± 0.03
R_{bg}^{fit}	0.141 ± 0.006	0.199 ± 0.006

Table 3
Breakdown of error sources

error source	δg_V	δg_A	$\delta \sin^2\theta$
statistics	0.012	0.006	0.0058
ν-beam composition	0.005	0.002	0.0026
ν-flux	0.006	0.009	0.0030
π°-Background	0.005	0.007	0.0025
ν_eN-Background	0.001	0.002	0.0008
incl. νN-Background	0.002	0.002	0.0007
detector resolution	0.006	0.005	0.0028
fit range	0.004	0.004	0.0019
selection efficiency	0.001	0.009	0.0007
Σ systematics	0.012	0.016	0.0059
total	0.017	0.017	0.0083

[1] F.J. Hasert et al., Phys.Lett.B46(1973)121

[2] CHARM Collab., F. Bergsma et al., Phys.Lett.B147(1984)481

[3] G. t'Hooft, Phys.Lett.B37(1971)195

[4] CHARM-II Collab. (P. Vilain et al.), Phys.Lett.B302(1993)351

[5] CHARM-II Collab. (P. Vilain et al), Phys.Lett.B320(1994)203

[6] CHARM-II Collab. (K. de Winter et al), Nucl.Inst. & Meth.A278(1989)670

[7] CHARM-II Collab. (D. Geiregat et al), Phys.Lett.B232(1989)539

[8] CHARM-II Collab. (D. Geiregat et al.), Phys.Lett.B259(1991)499

[9] CHARM-II Collab. (P. Vilain et al.), Phys.Lett.B281(1992)159

[10] CHARM-II Collab. (D. Geiregat et al.), Nucl.Instr. & Meth.A325(1993)92

[11] CHARM-II Collab., Th. Voss, PhD thesis Univ. of Hamburg 1993, unpublished

[12] CHARM-II Collab., L. Gerland, int. note (1989) unpublished

[13] The LEP Collab. : ALEPH, DELPHI, L3 and OPAL, Phys.Lett.B276(1992)247, and CERN-PPE/93-157, ALEPH CERN-PPE/94-30(Z Phys C), DELPHI CERN-PPE/ 94-31 (Nucl.Phys.B) and L3 CERN-PPE/94-45 (Z Phys C) and private communication from J. Mnich

[14] F. Reines, H. Gurr and H. Sobel, Phys.Rev.Lett.37(1976)315

[15] S.L. Wu, Proc.Int.Symp. Lepton and Photon Interactions at High Energies, ed. W. Bartel(1987)39

[16] V.A. Novikov, L.B. Okun and M.I. Vysotsky, Mod.Phys.Lett.A, Reviews, 8(1993)2529 and Errata 3301

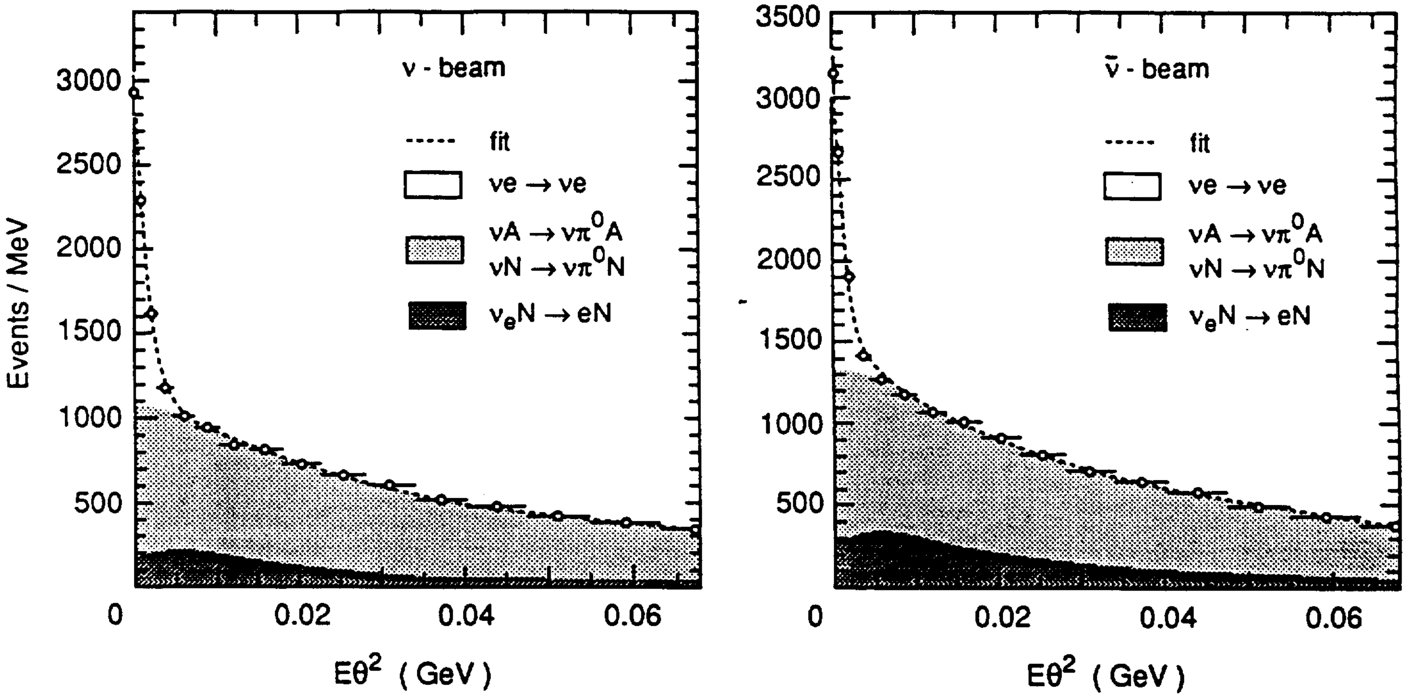

Figure 1 : Experimental data and the result of the best fit; data are shown as circles and the fit results are displayed as a dashed line. Only the projections in $E_e\theta_e^2$ of the 2-dim. distributions are shown. The different background components are added on top of each other. The bin size varies with the experimental resolution.

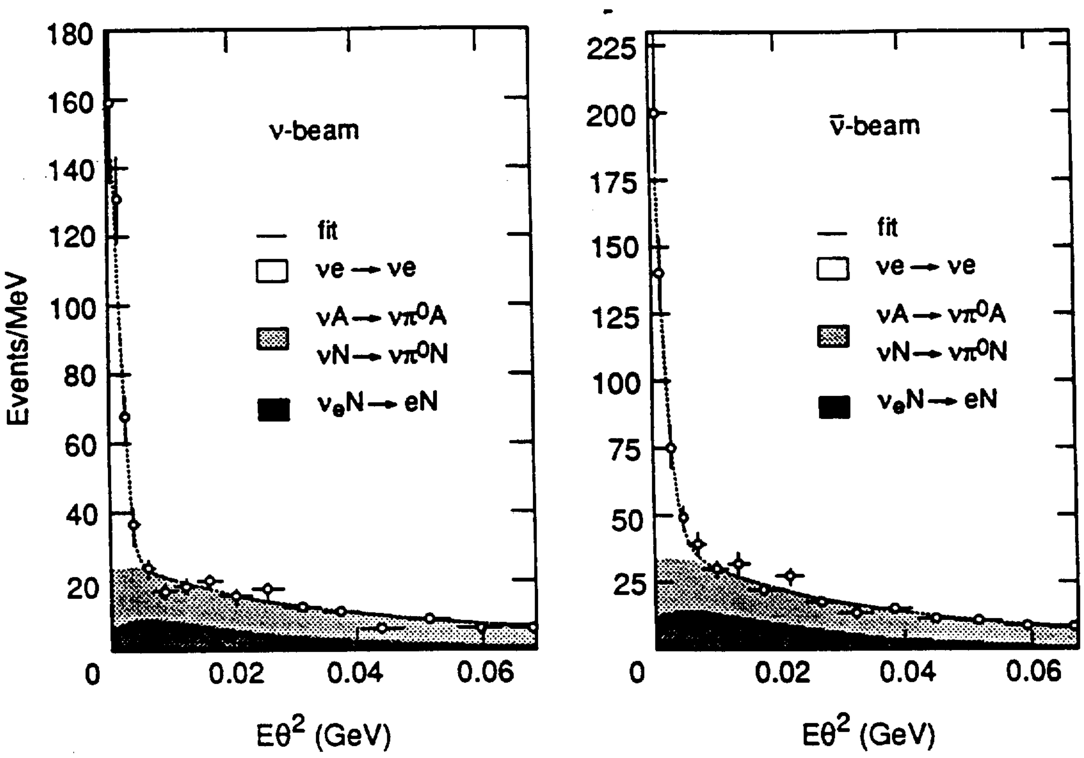

Figure 2 : Experimental data and the result of the best fit for the sample of events with energy loss information weighted with the electron probability. The signal to background ratio is improved by a factor 3.5 with respect to the total sample shown in figure 1. The bin size varies with the experimental resolution.

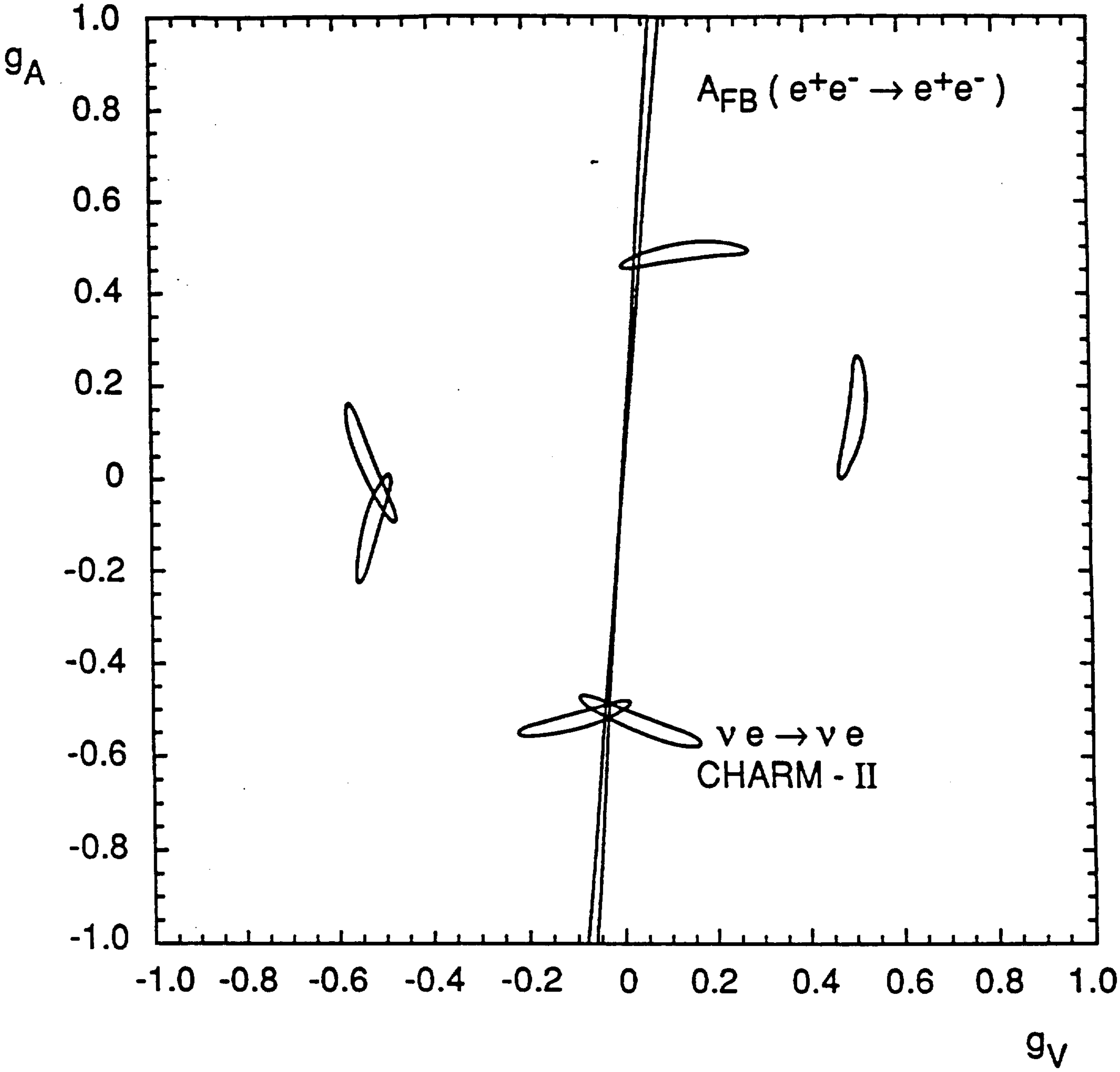

Figure 3 : 90% confidence level contours in the g_V–g_A plane, as obtained from the fit to the data from the ν–beam, the $\overline{\nu}$–beam and to both beams. Only statistical errors are considered. Results from experiments on the forward-backward asymmetry for $e^+e^- \to e^+ e^-$ at LEP [13] are shown as well. Together they select a single solution in agreement with $g_A^e = -1/2$.

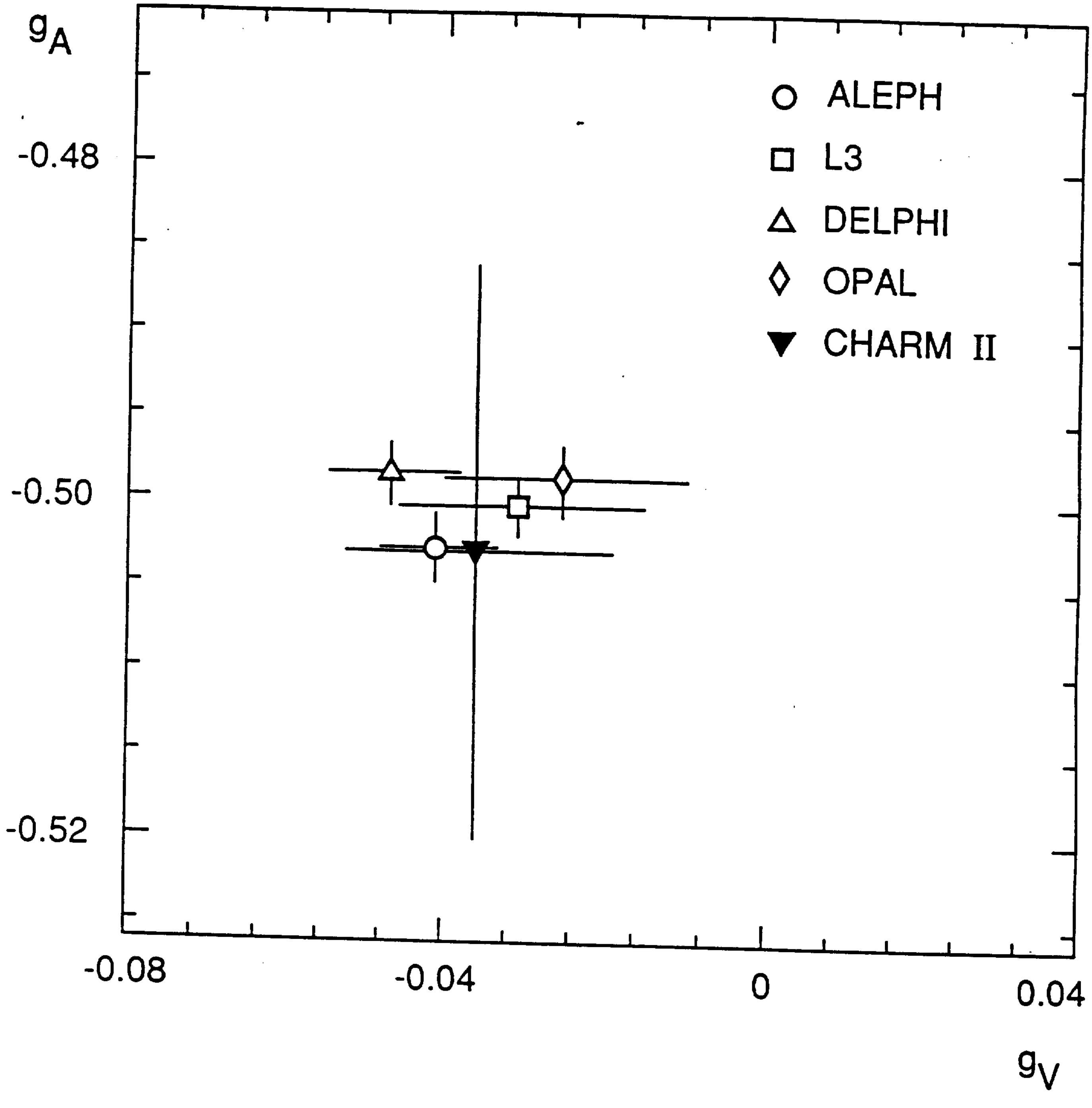

Figure 4 : Comparison of results from neutrino-electron scattering (this experiment) and measurements of the forward-backward asymmetry and of Γ_e for $e^+e^- \rightarrow e^+e^-$ annihilations at the Z° pole [13] in the g_V-g_A plane.